Interferometric studies of nearby galactic centers

Markus Wittkowski[a], Wolfgang J. Duschl[b], Karl-Heinz Hofmann[c], Alexander B. Men'shchikov[c], and Gerd Weigelt[c]

[a]European Southern Observatory, Casilla 19001, Santiago 19, Chile
[b]Institut für Theoretische Astrophysik, University of Heidelberg, Germany
[c]Max-Planck-Institut für Radioastronomie, Bonn, Germany

ABSTRACT

We discuss the potential of interferometric studies of nearby galactic nuclei with long-baseline interferometric facilities. Information on the morphology of galactic centers has so far been limited to angular sizes corresponding to the diffraction limit of 6–10 m class telescopes. Optical and near-infrared interferometry could in principle be used to reach significantly higher angular resolution, but has so far only been used for bright objects due to the small collecting areas of existing interferometers. Right now, the first interferometers consisting of 8–10 m class telescopes are starting operations and, hence, will soon allow us for the first time to study galactic centers on angular scales which are of an order of magnitude smaller than ever before, i.e. on scales corresponding to baselines of up to 100 m. We discuss these facilities and report on the observational techniques and strategies which are relevant for interferometric observations of these objects. We review imaging results of nearby galactic centers with highest angular resolution so far, with an emphasis on our bispectrum speckle interferometry studies of the core of the Seyfert galaxy NGC 1068. Employing these results, we analyze how near-infrared interferometry can discriminate between the different scenarios which are consistent with our current knowledge based on observations. In particular, characteristic sizes of the circumnuclear dusty torus can be derived with higher precision, additional dust components and the inner part of the jet can be identified, and radiative transfer models of the torus can be better constrained. Furthermore, the flux contribution of central source components can be separated from those of the torus, and thus they can be modeled in more detail. These investigations may ultimately result in a refinement of the unification scheme of galactic nuclei.

Keywords: active galactic nuclei, high-resolution astronomy, long-baseline interferometry, speckle interferometry

1. INTRODUCTION

High-resolution studies directly revealing the morphology of astrophysical objects are essential for our understanding of all areas of astrophysics, and have often been the key to milestone achievements (e.g. R 136, η Car). Whereas studies with angular resolutions of up to 1 mas have already routinely been achieved in radio astronomy by employing interferometric techniques with facilities like the VLBA (Very Large Baseline Array), large-aperture optical and infrared interferometers with long baselines are currently in the process of construction and commissioning. Several optical and infrared interferometers with relatively small collecting areas have been operated, starting with the pioneering works of Fizeau and Michelson, and are described in detail in these proceedings. The first construction of large interferometric facilities with 8–10 m class telescopes and baselines of up to the order of 100 m is currently in progress. These facilities include the Keck, VLT (Very Large Telescope), and LBT (Large Binocular Telescope) interferometers. Further interferometric beam combinations including 8–10 m apertures have been discussed, as for instance those between neighboring Mauna Kea telescopes (24, 25). These facilities with their large collecting areas will be the first instruments that allow us to study galactic centers with spatial resolutions of up to 1 mas at optical and infrared wavelengths. Except for maybe a very few brightest galactic centers, smaller aperture interferometers will not be sensitive enough. Using for instance a $B = 120$ m VLTI baseline, the resolution λ/B at $\lambda = 1.2\,\mu$m is 2 mas, i.e. about the same as currently achieved

E-mail: mwittkow@eso.org, wjd@ita.uni-heidelberg.de, hofmann@mpifr-bonn.mpg.de, sasha@mpifr-bonn.mpg.de, weigelt@mpifr-bonn.mpg.de

at radio wavelengths with VLBI. This unprecedented angular resolution will allow us to study nearby galactic centers at optical and infrared wavelengths in great detail. It is very difficult to predict what structures might be expected to be found, although this is crucial because model-specific assumptions will have to be made for the use of the limited feasible coverages of the *uv* plane with the VLT and Keck interferometers. Some clues on the structures one can observe can be obtained from high-resolution interferometric maps at radio wavelengths, from analyses of the observed spectra, and from the unified models of AGN (active galactic nuclei). Further important information on the expected visibility values at near-infrared wavelengths can be derived from present observations at the diffraction limit of the currently largest single-aperture 6–10 m class telescopes.

The main ingredient of the unified models is a geometrically and optically thick circumnuclear torus, which may obscure the central energy source, depending on the observer's viewing angle (see Antonucci[2] for a review). Such a torus would collimate radiation from the central source and lead to the observed ionization cone. Krolik & Begelmann[18] were the first to study dusty tori theoretically; other geometries have also been discussed, such as an extended disk consisting of several molecular clouds or a warped disk.

Here, we review the expected performance and potential of upcoming interferometric facilities, near-infrared observations of nearby active galactic nuclei with presently highest spatial resolutions, and the currently adopted unified models for the structure of AGN. With this information, we discuss which structures one can expect to observe, and how different scenarios can be constrained.

2. INTERFEROMETRIC TECHNIQUES AND FACILITIES

Until extremely large optical telescopes with diameters of the order of 100 m become available (see e.g., the concept study of the Overwhelmingly Large Telescope OWL[12 7]), optical and infrared studies with spatial resolution up to about 1 mas require the use of interferometers. Here, basic techniques and characteristics of different interferometers and their instruments are reviewed with respect to the observations of galactic centers.

Field of view. Two types of interferometric beam combinations have to be distinguished, the "Michelson" type and "Fizeau" type interferometers. The latter technique implies that the output pupil equals the input pupil or a scaled version of it for the whole integration time, so that the beams can interfere at the final (output) image plane. This configuration can most easily be achieved if all apertures share one mount, and the entrance pupil is constant for all pointing directions. Then, the field of view is limited only by the performance of the optical components, e.g. by the adaptive optics system. Such a configuration was chosen for the LBT interferometer, and a field of view of one arcminute or more is expected at near-infrared wavelengths (Herbst et al.[16]). The Michelson beam combination technique, as chosen for the Keck and VLT interferometers, is a configuration where input and output pupils are not equal, limiting the field of view to about 1 arcsec. It has the advantage of allowing longer baselines. With this technique, spatial filtering is often applied in order to improve the accuracy of the measured visibility values, which further limits the field of view to the size of one Airy disk. This field of view will usually be sufficient, since we are interested in the spatial scales which are not available with single telescopes at their diffraction limits. However, this limitation complicates consistent observation of both very compact structures and more extended environments, as expected for galactic centers. In addition, for objects which are not bright enough to allow adaptive optics and fringe tracking (most galactic centers) the limited field of view decreases the probability of finding a bright reference star within the field. To cope with this problem, the Michelson style interferometers can be equipped with a so-called "dual-feed facility" which allows the feeding of two fields into the beam combiner. The second field can then be chosen to include the reference star. The maximum separation of the two fields is again limited by the optical quality and, for the VLTI (PRIMA facility), it amounts to ~ 1 arcmin, comparable to the field of view of the Fizeau type interferometers.

Magnitude limit. The target itself or a nearby reference star within the isoplanatic patch and the field of view has to be bright enough to allow for adaptive optics and fringe tracking. The limiting K-band correlated magnitude for the planned interferometers consisting of 8–10 m class telescopes is about 12 mag. Only a very few cores of galactic centers will be brighter. For the interferometric observation of fainter targets, the use of a

Table 1. Cross-correlation of objects in the catalog "Quasars and Active Galactic Nuclei (8th Ed.)"[33] with objects in the Hipparcos catalog[26] within a distance of up to 1 arcmin. The table lists the name of the AGN, its redshift z, its type, its apparent V magnitude $V_{\rm AGN}$, its bolometric luminosity $M_{\rm bol}$, the distance to the Hipparcos star d, the Hipparcos catalog number HIP, the star's spectral type Sp.T., and its apparent V magnitude $V_{\rm Ref}$.

AGN Name	z	Type	$V_{\rm AGN}$	$M_{\rm bol}$	d (arcsec)	HIP number	Sp.T.	$V_{\rm Ref}$
MARK 1152	0.05	S1	15.0	-21.7	39.8	5756	F7V	9.60
0120-352	0.30		0.0	0.0	48.6	6433	K0III	8.23
PHL 1194	0.30		17.5	-23.9	49.2	8655	M...	8.10
B19.09	2.02		18.2	-27.8	58.9	9296	G8III	6.92
Q 0247+0214	0.20		18.4	-22.1	43.4	13234	F5	8.66
ESO 548-G81	0.02	S1	13.7	-21.1	45.6	17284	K0IV	8.40
PKS 0435-300	1.33		17.5	-27.4	29.2	21550	F5V	8.11
OK 568	0.57		18.6	-24.1	28.3	47818	K0	8.70
AH 26	2.21		18.6	-27.5	20.3	64269	K0III	8.44
ESO 325-IG22	0.04	S2	15.0	-21.8	44.2	67347	B9.5V	7.99
MS15498+2022	0.25		16.4	-24.6	56.0	77723	G	8.92
PKS 1551+130	1.29		17.7	-26.8	54.8	77830	F0	11.40
MS17462+6738	0.04	S1	15.7	-21.3	20.0	86957	K5	8.10

bright reference star for fringe tracking and adaptive optics will be mandatory. Table 1 lists all objects given in the catalog *Quasars and Active Galactic Nuclei (8th Ed.)*[33] that have a close reference star listed in the Hipparcos catalog[26] within a distance of 1 arcmin. Considering that the Hipparcos catalog is complete only up to $V \approx 9$ mag, while reference stars of up to $K \approx 12$ mag (i.e. $V > 12$) can be used, a considerably larger number of AGN with a nearby reference star will be available. Complete searches for these targets are very desirable and have already been initiated. These galactic centers which have a nearby reference star can then still be observed with a Fizeau-type interferometer (LBT) or with a Michelson-type interferometer which is equipped with a dual-feed system (e.g. VLTI with PRIMA). It is important to emphasize that the limiting magnitude of the instruments must be reached with the correlated flux of the objects within the field of view. For the example of the brightest Seyfert galaxy, NGC 1068, the K-band magnitude within an aperture of 5 arcsec was measured to be 7.3 mag (30). However, the K-band magnitude of the central core of NGC 1068, which would be measured by interferometers, might be as low as 8.8 mag (31) or even 9.3 mag (29). Since the innermost core structure is unknown, another considerable part of this magnitude of the core might be uncorrelated for baselines larger than ~ 10 m.

Imaging capabilities. The observables of an interferometer are the amplitude and phase of the complex visibility function, which is the Fourier transform of the object intensity distribution. In the presence of atmospheric turbulence, usually only the squared visibility amplitudes and the triple products are accessible by optical and near-infrared interferometers. The general methods of reconstructing an image from sparse aperture interferometric visibility data points have been developed by radio astronomers. A recent review describing the image fidelity using optical interferometers can be found in Baldwin & Haniff.[3] In order to reconstruct an image of reasonable fidelity, it is intuitively understandable that the number of visibility data points has to be at least as large as the number of unknowns, i.e. the pixel intensities of the image. Furthermore, despite the ability of imaging algorithms to effectively interpolate the sparse aperture data, the aperture has to be filled as uniformly as possible. Since interferometers consisting of 8–10 m apertures have to be used, and these interferometers are limited to 2–3 elements, only a limited coverage of the uv plane will be available, except the case of the LBT. This means that images with only a few pixels will be feasible for spatial resolutions corresponding to baselines larger than the LBT 23 m baseline. In this case, model fitting will be a better choice than imaging, but with the disadvantage that model assumptions will have to be made.

3. HIGH-ANGULAR RESOLUTION MEASUREMENTS OF NGC 1068

The Seyfert galaxy NGC 1068 harbors one of the brightest and closest AGN. Hence, it is one of the best studied galactic centers and observations of this object, combined with theoretical modeling and radiative transfer calculations, have substantially contributed to our current view of the structure of AGN. In particular, several studies with high angular resolution at the diffraction limit of the current 6–10 m class telescopes have been published for this object. The high-resolution information is reviewed here, in order to combine it with the unified models, and finally to estimate which structures one might expect to observe with higher angular resolutions.

HST observations with an angular resolution of ~ 0.1 arcsec were obtained in the UV continuum, the optical continuum and the [OIII] 501 nm emission line (19). These images show the narrow-line region, a conus-shaped structure in about N-S direction, with the central source obscured. Radio observations with similar angular resolutions were carried out starting with the work by Ulvestad et al.[32] These observations show several radio peaks in approximately NE-SW direction, of which only one ("S2") shows a positive spectral index α ($S_\nu \sim \nu^\alpha$), and is considered the position of the central core. The other emission peaks are interpreted as coming from the radio jet. The central source S2 was studied by Gallimore et al.[11] at 8.4 GHz with a very high angular resolution of ~ 1 mas, revealing a structure approximately perpendicular to the radio jet, which was interpreted as the emission of the torus that surrounds the central nucleus. Several near-infrared (NIR) and mid-infrared (MIR) studies aimed at searching for sub-arcsecond structures in the nuclear region of NGC 1068. Observations carried out by Neugebauer,[23] McCarthy,[22] Chelli et al.,[6] Thatte et al.,[31] Bock et al.,[5] and Weinberger et al.[35] are consistent with a compact (unresolved) central core, extended emission in approximately N-S direction out to $\sim$200 – 500 mas, and more extended structures. Rouan et al.,[29] Marco & Alloin,[21] Alloin et al.,[1] and Galliano & Alloin[10] report also on a ~ 80 pc (1.2 arcsec) E-W structure along position angle $\sim$102 deg, i.e. similar to the orientation of the 8.4 GHz radio continuum image, and interpret it as the dusty molecular torus at infrared wavelengths.

Recently, we presented the first diffraction-limited 76 mas resolution K-band bispectrum speckle interferometry observations of NGC 1068 (Wittkowski et al.[36]) resolving its ~ 30 mas (2 pc) nucleus. Figure 1 shows the

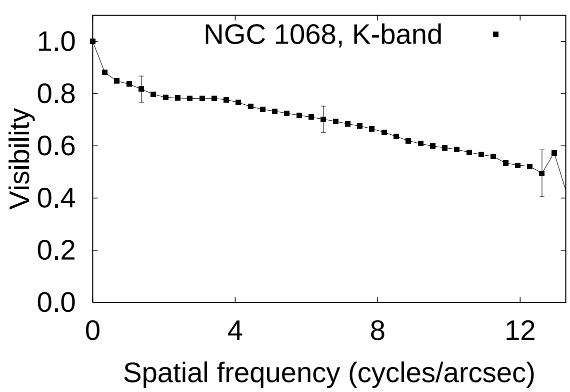

Figure 1. Azimuthally averaged K-band visibility (36) obtained by speckle interferometry at the SAO 6 m telescope, Russia.

azimuthally averaged NGC 1068 K-band visibility function based on the data shown by Wittkowski et al.,[36] which were obtained at the SAO 6 m telescope, Russia. The K-band visibility function shows a low-frequency visibility peak caused by extended emission and, at higher spatial frequencies, decreases monotonously up to the diffraction limit, corresponding to the maximum baseline of 6 m. Figure 2 shows the bispectrum speckle interferometry reconstruction of the K-band nucleus of NGC 1068 (from 36). An analysis of this image reveals that the nucleus is slightly resolved in all directions with azimuthally averaged diameter of ~ 30 mas for a well-fitting Gaussian intensity distribution. It shows a compact emission feature at PA ≈ -20 deg. The additional extended emission corresponding to the low-frequency visibility peak in Fig. 1 is not visible in this reconstruction.

The visibility function can also be used to separate the flux contributions from the extended and compact components. The following flux values were obtained based on the K-band data set discussed above, and a new

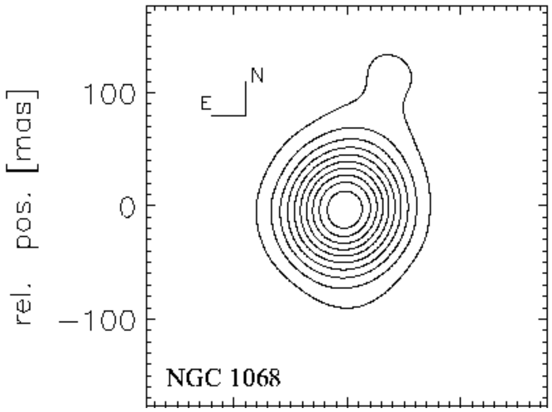

Figure 2. Bispectrum speckle interferometry reconstruction[36] of the K-band image of the nucleus of NGC 1068.

H-band dataset:

Dataset	Field of view	Flux within the field of view	Flux of the compact component
10/96 K-band	2×2 arcsec	650 ± 200 mJy	520 ± 210 mJy
09/99 H-band	3.9×3.9 arcsec	260 ± 100 mJy	76 ± 50 mJy

The separation of the compact component's flux contribution from the total observed flux at different wavelengths is important for the modeling of the circumnuclear torus. With the use of the upcoming interferometric facilities and their longer baselines, the flux of the compact component could further be decomposed into the contributions of the central nuclear source and of the compact resolved emission from the circumnuclear dusty torus (see below). The H and K magnitudes of the central source, in addition to usually available radio observations, are very important for testing and constraining models of this source, including for instance a non-thermal synchrotron source and thermal emission from an accretion disk.

4. INTERPRETATION OF THE OBSERVATIONS OF NGC 1068, AND VISIBILITIES AT HIGHER SPATIAL FREQUENCIES

In order to estimate the near-infrared visibility function of galactic nuclei at longer baselines, we consider the following simplified four-component model for the observed sub-arcsecond K-band emission, based on the observations of NGC 1068 as described above, results of published radiative transfer calculations, and standard unified models of AGN. Figure 3 illustrates this model.

- **A: The central source.** The emission from the nucleus may include for instance synchrotron radiation from electrons (as discussed by Wittkowski et al.[36] based on studies of our Galactic Center[4]), and radiation from a standard or advection-dominated accretion flow. Broad-line region clouds at very small distances of typically 2–20 mpc (determined by reverberation mapping and photoionization modeling, see eg. Wandel et al.[34]) may surround this nuclear source. The total nuclear spectrum likely extends to K-band. Some of these photons could reach us directly.

- **B: The inner sub-parsec part of the dusty molecular torus.** Hot dust in the innermost sub-parsec parts of the dusty torus emits thermal K-band photons. These photons can escape in a direction other than the equatorial plane, and can reach us directly.

- **C: Scattering dust clouds between BLR and NLR at distances of a few parsec from the center.** Dust clouds might exist in the region between broad-line region (BLR) and narrow-line region (NLR) at distances of only a few parsec from the nucleus, as suggested by Efstathiou & Rowan-Robinson[8] Efstathiou et al.[9] , and Hough.[17] Optically thin dust at this distance from the central source is unlikely to contribute significantly to fluxes emitted at near-infrared wavelengths, as the radiative equilibrium

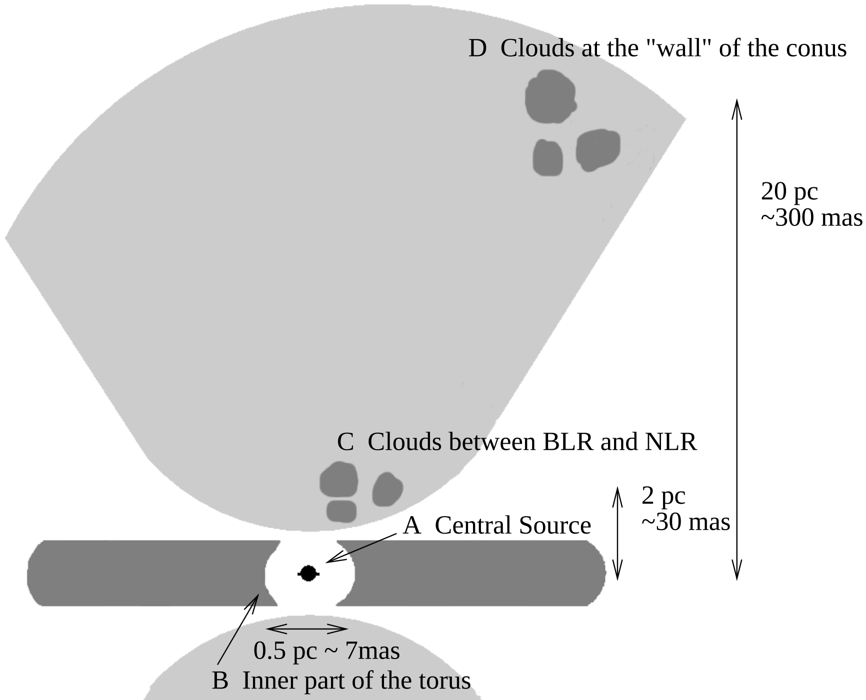

Figure 3. Sketch of the nuclear region of NGC 1068 (not to scale), including the central continuum source, the optically thick obscuring torus, optically thin dust clouds between broad line region and narrow line region above and below the torus, and narrow line region clouds within the ionization cone. K-band photons originate in the central continuum source, at the inner edge of the torus and in optically thin dust above the torus. Some of these photons reach us directly (unresolved flux fraction of the compact component), some via scattering at the dust clouds between BLR and NLR (compact component), and some via scattering at electrons and dust at the "wall" of the ionization cone (extended component).

dust temperature at the distance of the NGC 1068 nucleus is estimated to be ~ 500 K. However, this dust component can scatter near-infrared photons, which originate in the nucleus or the inner sub-parsec part of the dusty torus, i.e. in components **A** and **B**, into our line of sight.

- **D: Scattering electron and dust clouds at the "wall" of the ionization cone at distances of the order of 10 parsec from the center.** Scattering electron and dust clouds are expected to exist in the narrow-line region and at the wall of the ionization cone at distances of the order of 10 parsec to 100 parsec (e.g. 27, 28). These clouds are expected to scatter nuclear near-infrared photons into our line of sight.

These four components are sources of near-infrared radiation at four different characteristic length scales, that can be spatially resolved by interferometric measurements. At the distance of NGC 1068, these length scales correspond to the angular scales shown in Table 2. The compact NGC 1068 component with a diameter of 30 mas as revealed by our K-band bispectrum speckle interferomety reconstruction, is consistent with model component **C**, while the low-frequency peak in our visibility function is consistent with an extended model component **D**. Our visibility function decreases to only about 50% at the diffraction limit (maximum baseline of 6 m). Hence, additional model components **A** and **B** are also consistent with our measurements, if their combined flux contribution is less than 50% of the total flux within our field of view. If the visibility function in Fig. 1 is fitted by a model consisting of a Gaussian intensity distribution (component **C**) and additional unresolved components **A** and **B** emitting together 50% of the total flux, the size of component **C** will be ~ 45 mas instead of 30 mas (as derived for the model without **A** and **B**).

Table 2. Dimensions and angular scales of the four components adopted in our NGC 1068 model.

Component	Dimension (pc)	Angular scale (mas)
A	$<\approx 0.05\,\mathrm{pc}$	$<\approx 0.7$
B	0.5	7
C	2	30
D	10-100	150-1500

Implications of the NGC 1068 model on the visibility function at longer baselines. The relative flux contributions of components **A** to **D** are generally unknown, which leads to different predictions for the K-band visibility function of NGC 1068 for baselines beyond 6 m. Figure 4 shows a few possible predicted K-band visibility curves which are consistent with our current observational data. These simplified scenarios describe possible K-band extensions of the visibility function of NGC 1068, that has been measured only up to a baseline of 6 m. Similar visibility functions are expected for observations at shorter near-infrared wavelengths, with slightly different flux ratios and angular sizes of the different components. For galactic nuclei with different inclination angles, levels of activity, and luminosities, different sizes and flux contributions of these components are expected. The angular sizes of the different components scale with the distance, i.e. redshift, of a galaxy. The sizes and flux contributions of the different components can be studied for a variety of galactic nuclei by long-baseline interferometry. Sophisticated models can guide the analysis of multi-wavelength observations of the different nuclear components for a variety of galactic centers, as described in the following section.

5. DETAILED STUDIES USING MULTI-WAVELENGTH INTERFEROMETRIC MEASUREMENTS

The potential of interferometric measurements to separate the flux contributions of different components as described above, and to obtain their different characteristic scales will allow us to study these components in unprecedented detail. A few examples of feasible studies are outlined in the following.

Constraining radiative transfer models of the torus by multi-wavelength interferometric measurements. Interferometric measurements will enable the determination of angular scales of the dusty torus at different wavelengths, as well as the decomposition of the energy distribution of the torus emission. This information can then be compared with radiative transfer calculations, and properties of the torus can be derived. Presently, torus models with very different geometries are discussed. For instance for NGC 1068, a compact torus with a length scale of a few parsec and high optical depth was introduced by Pier & Krolik[27] .[28] Efstathiou & Rowan-Robinson[8] and Efstathiou et al.[9] use an extended torus model with a diameter of 180 pc. This model includes additional dust clouds between BLR and NLR at distances of a few parsec from the central source. Granato & Danese[14] and Granato et al.[15] discuss a thick torus model with a characteristic extension of 30 pc. Manske et al.[20] modeled AGN using a thick flared disk geometry and a strongly anisotropic central source. All torus models fit the observed mid-infrared SED of the nuclear region. Interferometric measurements will be able to constrain these models and to detect components in addition to the torus at this distance from the central source, as for example the suggested dust clouds between NLR and BLR, or the innermost infrared counterparts of the jet. These observations may also lead to a refinement of the torus concept resulting in more complex models.

Modeling of the central source. The spectral energy distribution at near-infrared wavelengths of the nucleus can be separated from flux contributions of extended components by interferometric measurements with baselines longer than 100 m for galactic centers at a distance of NGC 1068. Together with the usually available SED of the central source at radio wavelengths, the central energy production can be modeled in more detail including its possible anisotropy (Manske et al.[20]). For example, Wittkowski et al.[36] discussed possible implications of such measurements on the interpretation of the nuclear spectrum as optically thin synchrotron

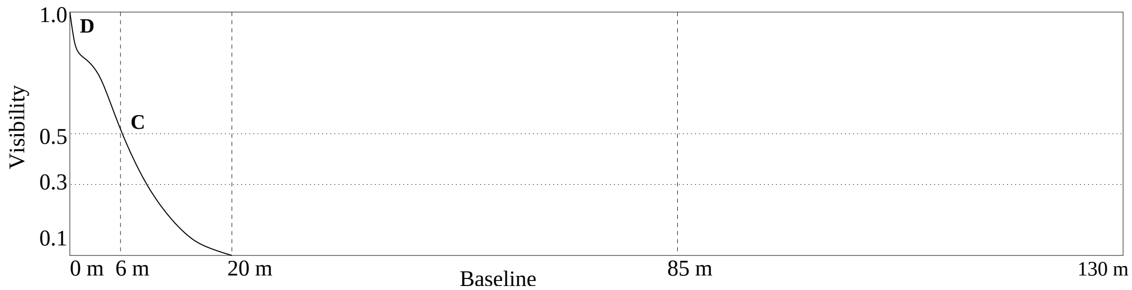

Components **C** and **D** completely obscure any more compact structures. The azimuthally averaged visibility function decreases monotonously to zero at a baseline of roughly 20 m, consistent with a symmetric Gaussian intensity distribution with FWHM of ≈ 30 mas.

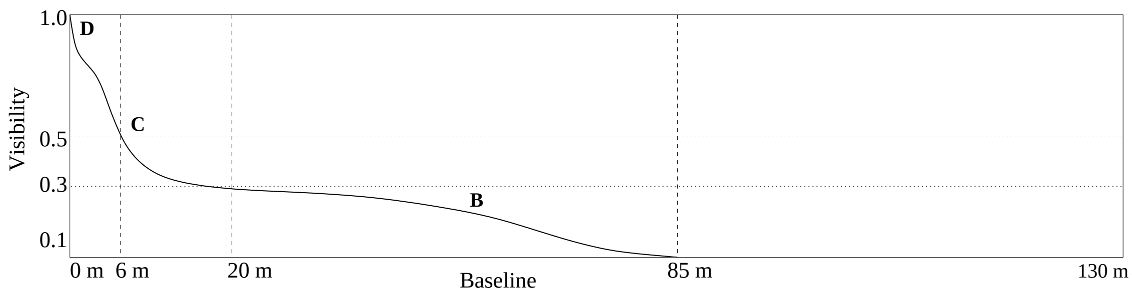

Component **B** has a flux contribution of 30% of the total flux, while component **A** is completely obscured. The visibility function flattens and transforms into a second Gaussian function which reaches zero at a baseline of roughly 85 m, corresponding to the 7 mas diameter of structure **B**.

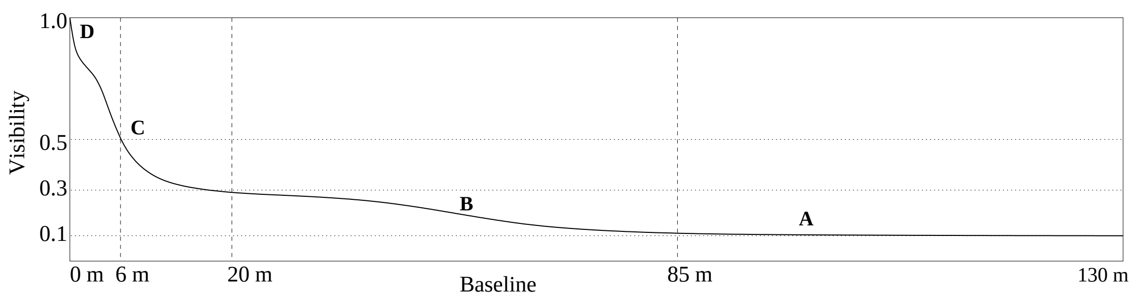

Component **B** has a flux contribution of 20% and component **A** has an additional flux contribution of 10%. The visibility function looks like the one before, but transforms into a constant or very slightly decreasing function at the 10% level for baselines longer than about 85 m.

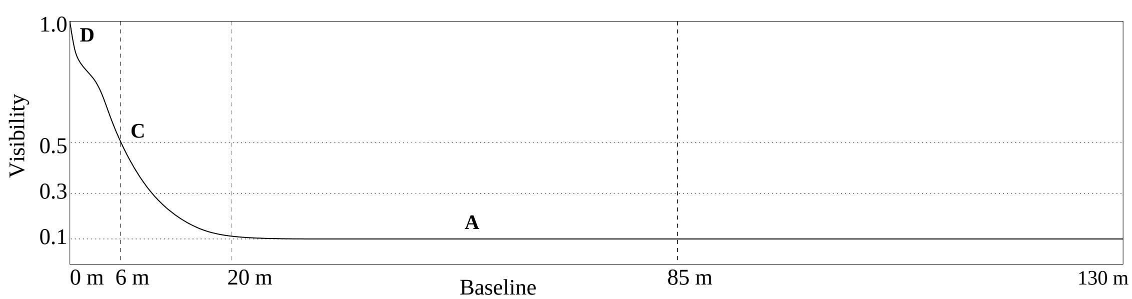

Component **B** is totally obscured (e.g. by the dusty torus), but component **A** is partly visible with a contribution of 10% of the total flux. The visibility function looks like the one before, but transforms into a constant or very slightly decreasing function at the 10% level for baselines longer than about 20 m.

Figure 4. Different predictions for the NGC 1068 K-band visibility function for baselines beyond 6 m.

.

radiation of quasi-monoenergetic electrons.[4] Additional nuclear source components may include emission from a standard or advection-dominated accretion flow or the innermost part of the jet. These sources are predicted to be surrounded by BLR clouds at distances of usually 2–20 mpc (as discussed above). These spatial scales are unresolved or marginally resolved for nearby galactic centers with baselines of 100 m. However, for a few cases, BLR sizes of up to 100 mpc are predicted by reverberation mapping. For a galactic center at the distance of NGC 1068, this size corresponds to an angular scale of $\approx$ 1mas, and a large BLR could be partially resolved with baselines of 100 m in the J-band.

Comparisons between galactic nuclei of different orientations, luminosities, and levels of activity. The studies as described above, i.e. the determination of characteristic length scales and SEDs of different central components, can be obtained for very different kinds of galactic centers. For example, as predicted by standard unified models of AGN, the inclination angle will have a significant impact on the observed flux contribution of the central source with respect to the total flux of the nuclear region. This information will constrain properties of the obscuring material. In addition, different levels of activity, and different luminosities will influence the characteristics of the different structures. These studies might also result in a better understanding of related phenomena, such as the AGN fueling mechanism or the AGN-starburst connection.

Galactic centers at different redshifts. The dependence on redshift of the characteristics of at least the compact component **C** and the extended component **D** can be investigated with next generation interferometers. Figure 5 shows the spatial scales of components emitted in K-band that can be resolved with a baseline of 120 m,

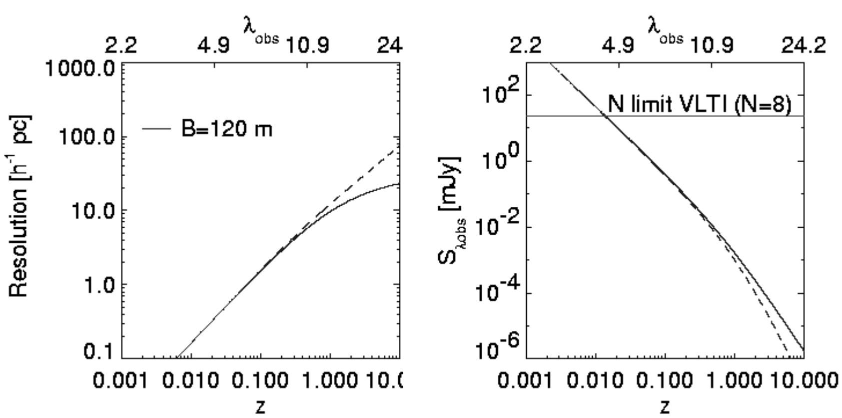

Figure 5. Absolute spatial scales (left) of components emitted in K-band that can be resolved with a baseline of 120 m (using $0.3\,\lambda/B$). Flux emitted in K-band (right) of a source with $F_K(z = 0.003) = 500$ mJy (NGC 1068) as a function of redshift. The observing wavelength is shifted to longer wavelengths with higher redshift. The solid lines denote a Einstein-de-Sitter world model (Ω_M=1) and the dashed lines a low density world model (Ω_M=0.05).

and the observed flux for NGC 1068 shifted to different redshifts. Observations of components emitted in K-band using current interferometers (VLTI and Keck) are limited by the observed flux at mid-infrared wavelenghts to a redshift of about 0.01–0.1. At this distance, structures with scales of about 1 pc can be resolved, which is of the order of the size of the compact component **B**. In order to perform these observations for a galactic center at redshift 1, it follows that an array consisting of 400 m apertures with baselines of up to 5 km is needed. This could for instance be realized by combining the light from several OWL type telescopes equipped with next generation detectors by optical fibers. Such a configuration has previously been discussed by Glindemann et al.[13] and called "La OLA" (Overwhelmingly Large Array). K-band observations of $\sim$ 5 pc components emitted at shorter wavelengths are already feasible with the current interferometers up to a redshift of $\sim$ 1.

REFERENCES

1. D. Alloin, E. Galliano, J.G. Cuby, O. Marco, D. Rouan, Y. Clenet, G.L. Granato, A. Franceschini, "Kinematics of molecular gas in the nucleus of NGC 1068, from H2 line emission observed with the VLT", *A&A* **369**, L33

2. R. Antonucci, “Unified models for active galactic nuclei and quasars”, *ARA&A* **31**, 473, 1993
3. J.E. Baldwin, C.A. Haniff, “The application of interferometry to optical astronomical imaging”, *Phil. Trans. A* **360**, 969, 2002
4. T. Beckert, W.J. Duschl, P.G. Mezger, R. Zylka, “Anatomy of the Sagittarius A complex. V. Interpretation of the SGR A* spectrum”, *A&A* **307**, 450, 1996
5. J.J. Bock, K.A. Marsh, M.E. Ressler, M.W. Werner, “High-Resolution Mid-Infrared Imaging of the Nucleus of NGC 1068”, *ApJ* **504**, L5, 1998
6. A. Chelli, I. Cruz-Gonzalez, L. Carrasco, C. Perrier, “High spatial resolution IR observations and variability of the nuclear region of NGC 1068 - Structure and nature of the inner 100 parsec”, *A&A* **177**, 51, 1987
7. P. Dierickx, R. Gilmozzi, “Progress of the OWL 100 m Telescope Conceptual Design”, *Proc. SPIE* **4004**, 290, 2000
8. A. Efstathiou, M. Rowan-Robinson, “Dusty discs in active galactic nuclei”, *MNRAS* **273**, 649, 1995
9. A. Efstathiou, J.H. Hough, S. Young, “A model for the infrared continuum spectrum of NGC 1068”, *MNRAS 277*, 1134, 1995
10. E. Galliano, D. Alloin, “Near-IR 2D-Spectroscopy of the 4”x4” region around the Active Galactic Nucleus of NGC 1068 with ISAAC/VLT”, *A&A* 2002, astro-ph 0207010
11. J.F. Gallimore, S.A. Baum, C.P. O’Dea, “A direct image of the obscuring disk surrounding an active galactic nucleus”, *Nature* **388**, 852, 1997
12. R. Gilmozzi, “Science with 100-m telescopes”, *Proc. SPIE* **4005**, 2, 2000
13. A. Glindemann, et al., “Growing up - the completion of the VLTI”, in *Scientific Drivers for ESO Future VLT/VLTI Instrumentation*, J. Bergeron, G. Monnet (eds.), 2001
14. G.L. Granato, L. Danese, “Thick Tori around Active Galactic Nuclei - a Comparison of Model Predictions with Observations of the Infrared Continuum and Silicate Features”, *MNRAS* **268**, 235, 1994
15. G.L. Granato, L. Danese, A. Franceschini, “Thick Tori around Active Galactic Nuclei: The Case for Extended Tori and Consequences for Their X-Ray and Infrared Emission”, *ApJ* **486**, 147, 1997
16. T.M. Herbst, H.-W. Rix, P. Bizenberger, M. Ollivier, “LINC: a near-infrared beam combiner for the Large Binocular Telescope”, *Proc. SPIE* **4006**, 673, 2000
17. J.H. Hough, “Infrared Polarimetry and the Torus”, *Ap&SS*, **248**, 269, 1997
18. J.H. Krolik, M.C. Begelman, “Molecular tori in Seyfert galaxies - Feeding the monster and hiding it”, *ApJ* **329**, 702, 1988
19. F. Macchetto, A. Capetti, W.B. Sparks, D.J. Axon, A. Boksenberg, “HST/FOC imaging of the narrow-line region of NGC 1068”, *ApJ* **435**, L15, 1994
20. V. Manske, T. Henning, A.B. Men’shchikov, “Flared dust disks and the IR emission of AGN”, *A&A* **331**, 52, 1998
21. O. Marco, D. Alloin, “Adaptive optics images at 3.5 and 4.8 μm of the core arcsec of NGC 1068: more evidence for a dusty/molecular torus”, *A&A* **353**, 465, 2000
22. D.W. McCarthy, F.J. Low, S.G. Kleinmann, F.C. Gillett, “Infrared speckle interferometry of the nucleus of NGC 1068”, *ApJ* **257**, L7, 1982
23. G. Neugebauer, G. Garmire, G.H. Rieke, F.J. Low, “Infrared Observations on the Size of NGC 1068”, *ApJ* **166**, L45, 1971
24. J. Nishikawa, K. Sato, T. Fukushima, M. Yoshizawa, Y. Machida, Y. Honma, “MIRA-II, MIRA-III, and MIRA-SG projects: the future plan of long-baseline optical/IR interferometers in Japan”, *Proc. SPIE* **3350** 184, 1998
25. G. Perrin, O. Lai, P.J. Lena, V. Coude du Foresto, “Fibered large interferometer on top of Mauna Kea: OHANA, the optical Hawaiian array for nanoradian astronomy”, *Proc. SPIE* **4006**, 708, 2000
26. M.A.C. Perryman, ESA, “The HIPPARCOS and TYCHO catalogues. Astrometric and photometric star catalogues derived from the ESA HIPPARCOS Space Astrometry Mission”, *ESA SP Series Vol. No. 1200*, 1997
27. E.A. Pier, J.H. Krolik, “Infrared spectra of obscuring dust tori around active galactic nuclei. I - Calculational method and basic trends”, *ApJ* **401**, 99, 1992

28. E.A. Pier, J.H. Krolik, "Infrared Spectra of Obscuring Dust Tori around Active Galactic Nuclei. II. Comparison with Observations", *ApJ* **418**, 673, 1993
29. D. Rouan, F. Rigaut, D. Alloin, R. Doyon, O. Lai, D. Crampton, E. Gendron, R. Arsenault, "Near-IR images of the torus and micro-spiral structure in NGC 1068 using adaptive optics", *A&A* **339**, 687, 1998
30. N.Z. Scoville, K. Matthews, D.P. Carico, D.B. Sanders, "The stellar bar in NGC 1068", *ApJ* **327**, L61, 1988
31. N. Thatte, A. Quirrenbach, R. Genzel, R. Maiolino, M. Tecza, "The Nuclear Stellar Core, the Hot Dust Source, and the Location of the Nucleus of NGC 1068", *ApJ* **490**, 238, 1997
32. J.S. Ulvestad, S.G. Neff, A.S. Wilson, "Radio structure in the inner 1 arcsecond of NGC 1068", *AJ* **93**, 22, 1987
33. M.P. Veron-Cetty, P. Veron, "Quasars and Active Galactic Nuclei (8th Ed.)", *VizieR On-line Data Catalog: VII/207*, 1998
34. A. Wandel, B.M. Peterson, M.A. Malkan, "Central Masses and Broad-Line Region Sizes of Active Galactic Nuclei. I. Comparing the Photoionization and Reverberation Techniques", *ApJ* **526**, 579, 1999
35. A.J. Weinberger, G. Neugebauer, K. Matthews, "Diffraction-limited imaging and photometry of NGC 1068", *AJ* **117**, 2748, 1999
36. M. Wittkowski, Y. Balega, T. Beckert, W.J. Duschl, K.-H. Hofmann, G. Weigelt, "Diffraction-limited 76 mas speckle masking observations of the core of NGC 1068 with the SAO 6 m telescope", *A&A* **329**, L45, 1998